Effect of additional silicon on titanium/4H-SiC contacts properties*

Zhang Yong-Ping(张永平), Chen Zhi-Zhan(陈之战)†, Lu Wu-Yue (卢吴越),
Tan Jia-Hui(谈嘉慧), Cheng Yue(程 越), and Shi Wang-Zhou(石旺舟)

Shanghai Normal University, Shanghai 200234, *China*

(Received 9 October 2013; revised manuscript received 23 December 2013; published online 25 March 2014)

The Ti electrode was deposited on the $(000\bar{1})$ face of an n-type 4H-SiC substrate by magnetron sputtering. The effect of the electrode placement method during the annealing treatment on the contact property was carefully investigated. When the electrode was faced to the Si tray and annealed, it showed ohmic behavior, otherwise it showed a non-ohmic property. X-ray diffraction (XRD), X-ray photoelectron spectroscopy (XPS), scanning electron microscopy (SEM), and atomic force microscopy (AFM) were used to characterize the electrode phase, composition, thickness, and surface morphology. The additional silicon introduced from the Si tray played a key role in the formation of the ohmic contact on the Ti/4H-SiC contact.

Keywords: Ti/4H-SiC, ohmic contact, surface morphology, additional silicon

PACS: 73.40.Cg, 68.55.–a **DOI:** 10.1088/1674-1056/23/5/057303

1. Introduction

Silicon carbide (SiC) is regarded as an excellent candidate for high power, high frequency, and high temperature electronic devices due to its excellent physical properties such as a wide band gap, high breakdown field, high thermal conductivity, and high saturation electron velocity.[1,2] One of the most active fields in SiC research is the development of electronic devices capable of functioning at high power and frequency, high temperature, and in caustic circumstances. The relatively high contact resistivity may cause an inadmissible voltage drop on the contacts due to the high current density. The ohmic contact is therefore a critical factor that could restrict the SiC device applications.[3]

The ohmic contact to n-type SiC was formed by the deposition of different metals or metal alloys.[4–6] Among them, Ti and Ti alloys were extensively studied.[7–9] Au/Ti ohmic contact on the $(000\bar{1})$ of n-type SiC was prepared, in which C atoms, released from SiC substrate, reacted with Ti atoms to form TiC at the contact interface.[10] Ti–Al contact was investigated and the ohmic contact property was ascribed to the formation of the ternary compound Ti_3SiC_2.[11–14] On the other hand, the morphology of the annealed metal contact often became rough due to intermixing and/or alloying after the high temperature annealing.[15] A rough silicide interface increased the high leakage of the shallow junctions.[16] Good ohmic contact with both low contact resistance and smooth surface morphology was required to develop a robust manufacturing process of high power, high frequency devices.

In this paper, we prepared Ti contacts on the $(000\bar{1})$ face of n-type 4H-SiC substrates. The Ti/4H-SiC interface reactions, contact resistance, and surface morphology were compared as responding to the different electrode placement methods for annealing treatment. The additional silicon introduced from the Si tray resulted in not only the smooth surface morphology but also the good ohmic contact property.

2. Experiment

The 4° off axis, n-type 4H-SiC substrate, with a doping concentration of about 1×10^{17} cm^{-3}, was used in this study. Prior to deposition, the substrates were ultrasonically cleaned in deionized water for 600 s to wipe off large particle contamination introduced by the process of dicing the wafer. They were then ultrasonically washed in alcohol: acetone (1:1) for 600 s to erase the organic contamination. The next step was performed with a boiled solution of H_2O: H_2SO_4(10:1) for 1500 s to remove the metal ions contamination. Finally, all the substrates were immersed in 10% HF for 1500 s, followed by large amounts of deionized water rinse to eliminate the oxide layers.

Ti electrodes were deposited on the SiC substrates by a magnetron sputtering system (ULVAC, Japan). Before deposition, the substrates were etched for 30 min by plasma to remove the native surface oxide on the SiC. The depositions were carried out at a constant pressure of 0.46 Pa in an Ar atomsphere for 3600 s. The substrate temperature was 300 °C.

The electrodes were annealed at 1000 °C for 180 s in an Ar atmosphere in a rapid thermal processing system (RTP 600). The tray to place the as-deposited samples was a 4-inch-silicon wafer (hereafter designated as the Si tray). Figure 1 is the schematic diagram of the placement method of as-deposited samples in the annealing treatment. The as-deposited sample was named S1. The samples with their electrodes facing and facing away from the Si tray were named S2

*Project supported by the National Basic Research Program of China (Grant No. 2012CB326402), the Innovation Program of Shanghai Municipal Education Commission, China (Grant No. 13ZZ108), and the Shanghai Science and Technology Commission, China (Grant No. 13520502700).

†Corresponding author. E-mail: chenwbgs@126.com

© 2014 Chinese Physical Society and IOP Publishing Ltd

and S3, respectively.

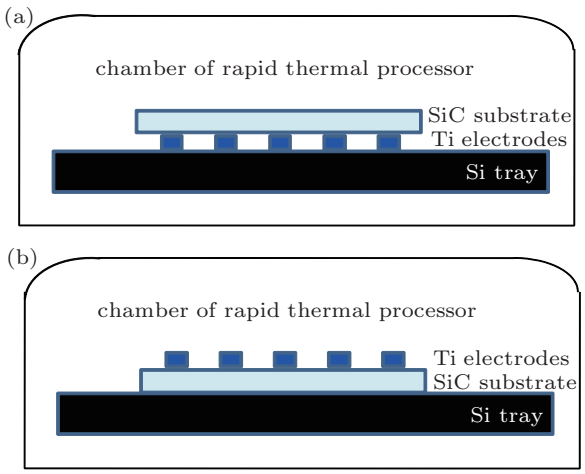


Fig. 1. (color online) The schematic diagram of the placement method of Ti/4H-SiC samples in the annealing treatment. (a) S2 with its electrode facing the Si tray, and (b) S3 with its electrode facing away from the Si tray.

The current–voltage (I–V) curves were measured by the Hall measurement system (Lakeshore 7704). The electrode phase was identified by X-ray diffraction (Bruker D8 Advance). The surface elemental composition was measured by X-ray photoelectron spectroscopy (PHI 5000). Photoelectron peaks were accurately curve-fitted by means of the PHI multipak software. The surface and cross-section morphologies were characterized by a Bruker atomic force microscope (Nanoscope III a) and scanning electron microscopy (Hitachi S-4800), respectively.

3. Results and discussion

Electrical properties of the as-deposited (S1) and annealed (S2, S3) samples are characterized by the current–voltage (I–V) curve. The S1 shows no ohmic behavior (Fig. 2(a)). However, when annealing treatment at 1000 °C is performed, the S2 is ohmic (Fig. 2(b)) while rectifying behavior is observed for S3 (Fig. 2(c)). The linear transmission line model (TLM) was used to calculate the specific contact resistance ρ_c of S2.[17,18] Definition of the contact pads for the TLM measurement was performed using a reactive ion etching (RIE) system with a 1-μm thick silicon dioxide etching mask. TLM structure was composed of six 900 μm×900 μm square Ti electrodes separated by 100 μm, 150 μm, 200 μm, 250 μm, and 300 μm, respectively. The plot of $R_{\rm Total}$ to contact resistance as a function of L is shown in Fig. 2(d). The ρ_c is 1.23×10^{-6} Ω· cm^2.

Figure 3 is the SEM cross-section and AFM surface morphologies for the three samples. The electrode is about 100-nm thick for S1. After annealing, the electrode thicknesses of S2 and S3 are increased to 118 nm and 130 nm, respectively. From AFM observation, the S1 exhibits a quite flat surface with a root-mean-square (RMS) of 0.998 nm (10 μm×10 μm), this RMS is slightly increased to 1.919 nm for S2. As for the S3, a significant increase in the RMS up to a value of 17.968 nm is measured.

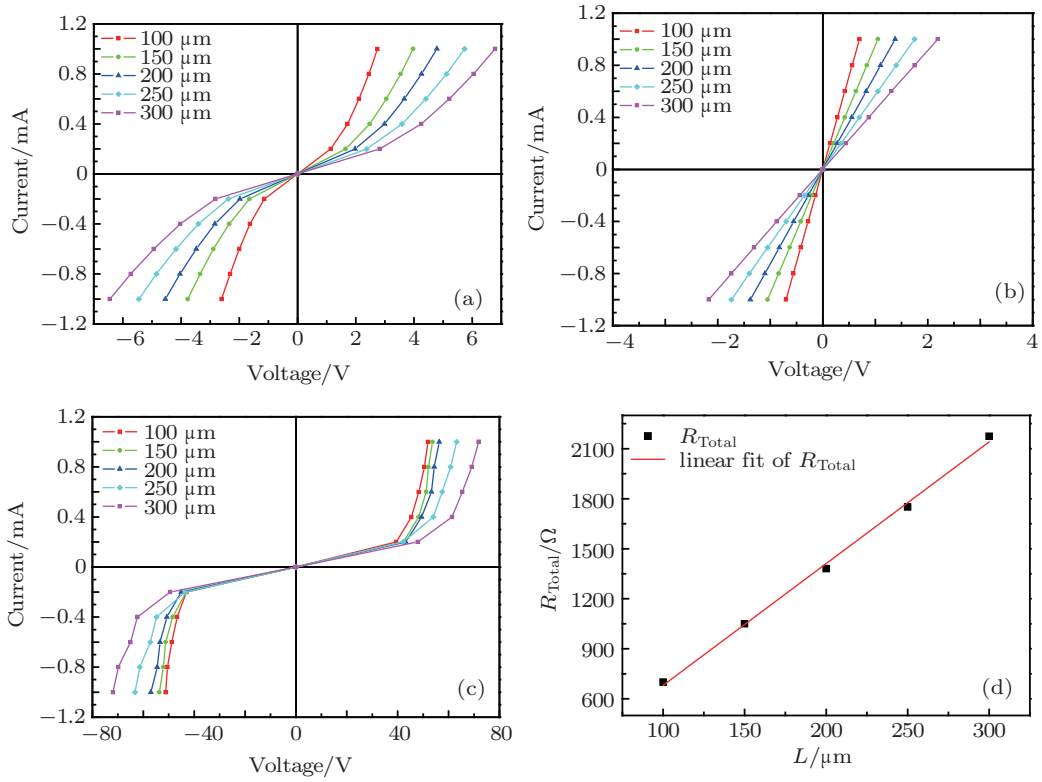


Fig. 2. (color online) The I–V characteristics of Ti contact onto (0001) C-face 4H-SiC. Panels (a)–(c) are for samples (a), (b), and (c) (S1, S2, and S3), respectively. (d) The plot of the contact resistance $R_{\rm Total}$ as a function of L for sample (b). The specific contact resistance ρ_C was calculated according to $\rho_C = LL_TR_C$, where R_C is the contact resistance, L_T is the transfer line length, and L is the electrode length.

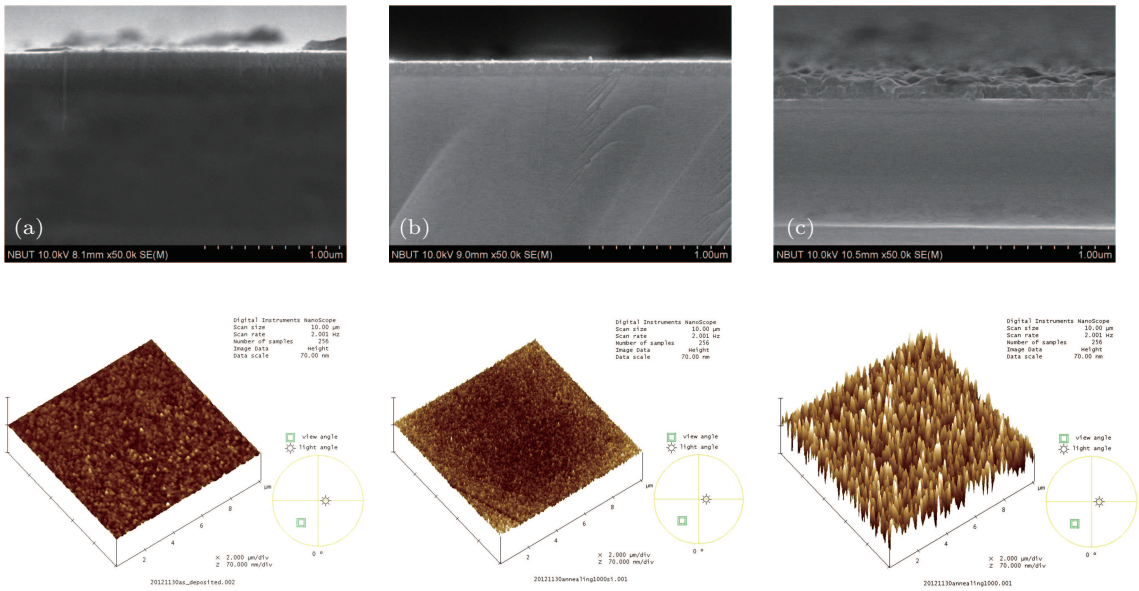


Fig. 3. (color online) SEM cross-sections and AFM surface morphologies of Ti/4H-SiC contacts for three samples. Panels (a)–(c) were for S1, S2, S3, respectively.

Figure 4 is the XRD patterns for S2 and S3. The positions of the diffraction peaks of these two samples are similar. The TiC (111), (200) diffraction peaks are identified. The SiC (004) overlapped with the TiC (111) at diffraction peak 35.9°. The extra peaks at 31° and 36.8° are attributed to the Ti_3SiC_2 and $Ti_5Si_3C_x$ phases, respectively. The TiC (200) overlaps with the Ti_3SiC_2 (008) at diffraction peak 41.1°.[19–21] In spite of TiC and Ti_3SiC_2 phases are identified in the samples, the peak intensities for S2 are higher than those of S3, especially for those of Ti_3SiC_2 peaks. The results suggested that more percentages of the Ti_3SiC_2 in S2 are generated.

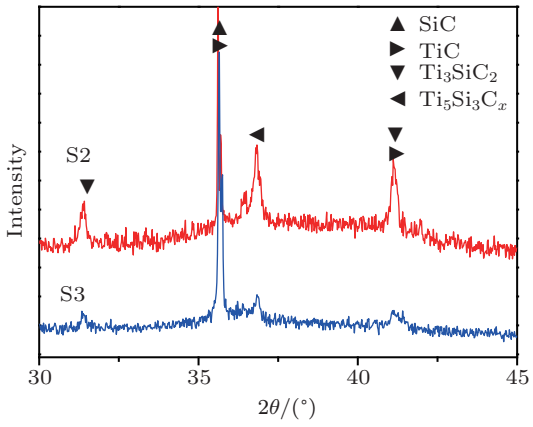


Fig. 4. (color online) XRD patterns of S2 and S3. Both electrodes are annealed at 1000 °C for 180 s.

Figure 5 is the XPS spectra for S2 and S3. Analyses of the C1s, Si2p, and Ti2p photoelectrons show that the S2 and S3 electrodes exhibit C–Ti interaction, with the C1s peaks located at 282.70 eV. From the Si2p spectrum, we obtain binding energies of 99.89 eV and 99.59 eV, due to the small escape depths of the photoelectron, the Si2p spectrum should be dominated by the surface layer, which is likely to be incomplete and has Ti atoms only on one side, so the obtained binding energy for Si2p may differ from the bulk value.[14] A smaller C–Si bonding at 282.9 eV is present, as observed from the convoluted spectra. The Ti2p chemical bonding energies are determined to be 454.5 eV for $Ti2p_{3/2}$, and 460.5 eV for $Ti2p_{1/2}$, which correspond to Ti–C bonding as in TiC.[21,22] The electrode surface elemental compositions of C, Si, and Ti are calculated from the XPS peak areas and standard relative sensitivity factors. The C, Si, and Ti atomic concentrations are 33.74%, 12.52%, 53.74% for S2, and 35.12%, 9.66%, 55.22% for S3, respectively.

It is almost impossible to form an ohmic contact relying only on the choice of a metal with suitable work function and metal diffusion into the SiC during annealing. In order to form an ohmic contact, metallization schemes are chosen so as to form an intermediate layer at the Ti/SiC interface, which could decrease the barrier height ($q\Phi_{Bn}$). In these cases, annealing treatment regenerates new interfacial compounds, the old Ti/SiC interface is eliminated and replaced by a new one. The resulting $q\Phi_{Bn}$ is not dependent on the SiC surface property and/or Ti work function. Based on the experimental results, the placement method of the electrodes in the annealing treatment plays a key role in the ohmic contact formation, which reveals an important insight into Ti/SiC contact. The formation process of the intermediate phases is described as follows.

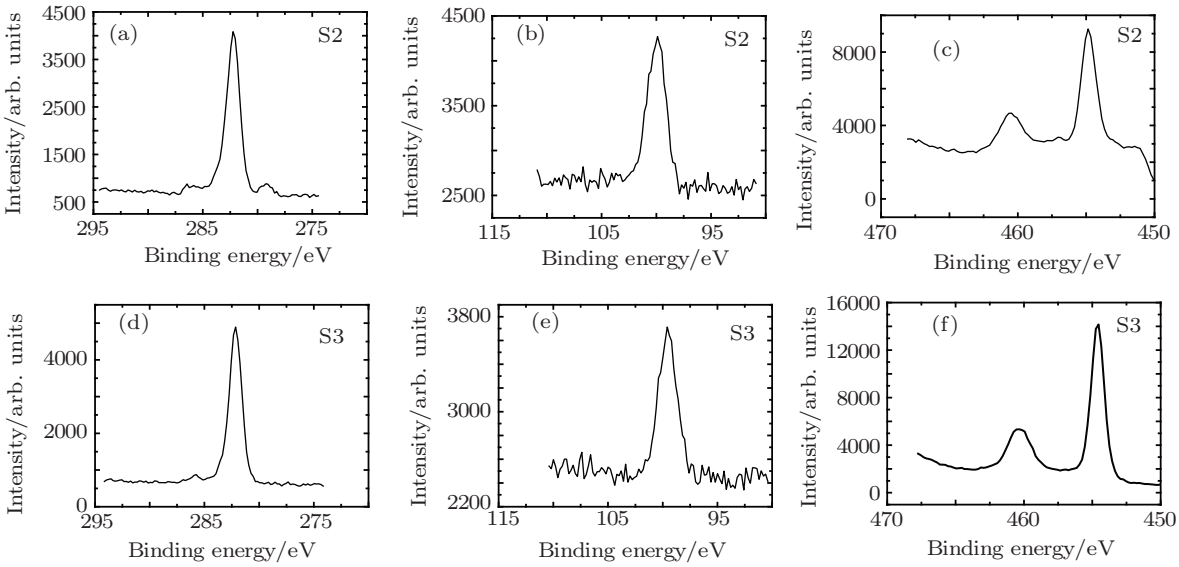


Fig. 5. XPS spectra of S2 and S3. Panels (a)–(c) are the C1s region, Si 2p region, and Ti2p region for S2, respectively; panels (d)–(e) are the C1s region, Si 2p region, and Ti2p region for S3, respectively.

It was reported that 1000 °C annealing caused SiC partial dissociation to form Si and C atoms.[23] The contact formation was initiated by the dissociation of the SiC surface, due to the high affinity of Ti for C at this temperature.[24] TiC and $Ti_5Si_3C_x$ at the Ti/SiC interface are generated by reacting Ti with SiC for S3 sample

$$Ti + C \rightarrow TiC, \tag{1}$$

$$5Ti + 3Si + xC \rightarrow Ti_5Si_3C_x. \tag{2}$$

At the interface Ti atoms diffuse into and through the TiC and $Ti_5Si_3C_x$ mixed layer towards the SiC side. Simultaneously, Si and C atoms diffuse towards the Ti side. Once a pileup of excess C atoms at the interface reaches the saturation limit for Ti_3SiC_2, a Ti_3SiC_2 phase is formed

$$3Ti + Si + 2C \rightarrow Ti_3SiC_2. \tag{3}$$

The supply of Ti atoms at the SiC side continues and the above reactions are repeated. On the other hand, more TiC phases are formed through reaction (1) at the Ti side since the diffusion of C atoms is faster than that of Si atoms. Finally, the deposited Ti layer is completely consumed, the new interfacial compounds are formed, as shown in Fig. 6(a).

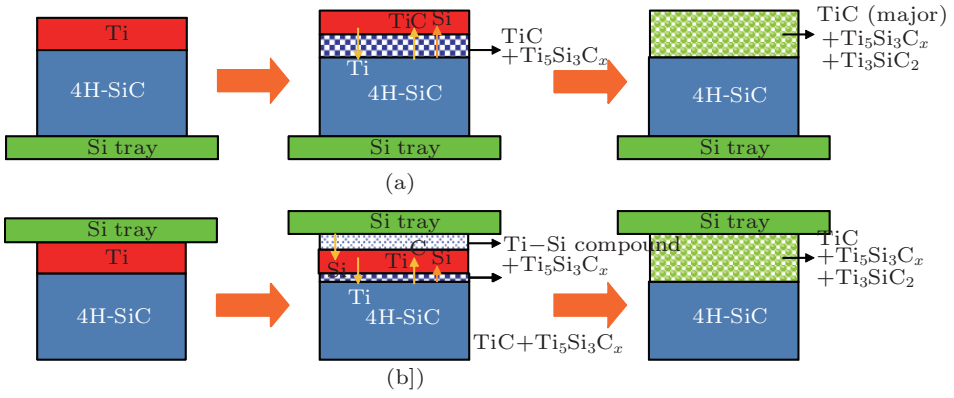


Fig. 6. (color online) The illustration of reaction pathway of S2 (a) and S3 (b).

In the case of S2, the Ti electrode is faced to the Si tray, the annealed system can be regarded as Si/Ti/SiC, as shown in Fig. 6(b), where Si refers to the Si tray. On the one hand, the TiC, $Ti_5Si_3C_x$, and Ti_3SiC_2 phases are formed at the Ti/SiC interface similar to that of S3 after annealing treatment. As the bonding energy for Si–Si bond in Si and Si–C bond in SiC are 1.81 eV and 4.47 eV, respectively,[25] the bond cleavage of Si–Si is easier than that of Si–C. When Si is introduced in the system, a part of dissociated Si atoms from the Si tray diffuse into the Ti layer to form a Ti–Si compound although

no Ti–Si phase is detected in the XRD pattern. When the C atoms dissociate from SiC diffuse into the Ti–Si compound layer, $Ti_5Si_3C_x$ and Ti_3SiC_2 are formed.

$$\text{Ti} - \text{Si compound} + \text{C} \rightarrow \text{Ti}_5\text{Si}_3\text{C}_x + \text{Ti}_3\text{SiC}_2. \quad (4)$$

To achieve good ohmic contact, $q\Phi_{\text{Bn}}$ between metal and semiconductor is required to be as low as possible for high current conduction.[16] After annealing at 1000 °C, TiC alloy compound is identified in S2 and S3 samples. As the work function of TiC (3.74–3.94 eV)[26] is smaller than that of Ti (4.33 eV),[27] leading to a reduction of $q\Phi_{\text{Bn}}$, which may be responsible for the decrease in contact resistivity of Ti/4H-SiC.

The above mentioned formation mechanism was verified by XPS data. The C, Si, and Ti atomic concentrations were 33.74%, 12.52%, and 53,74% in the S2 sample, and 35.12%, 9.66%, and 55.22% in the S3 sample, respectively. The percentages of Si was 2.86% more and C 1.48% less in the S2 sample than those in the S3 sample. This difference was caused by the different bonding energies of the Si–Si bond in Si and the Si–C bond in SiC. When the S2 was annealed, the Si atoms dissociation from the Si tray diffused into the Ti electrode, which weakened the diffuse driving force of Si atoms dissociation from the SiC substrate to Ti electrode. Therefore, the dissociation of SiC was suppressed to some extent. The effect of the annealing treatment on the electrode surface RMS and the thickness of the electrode were smaller. Compared with the S1 sample, the RMS and thickness increases were only 0.9 nm and 18 nm, respectively. Different from the S2 sample, no additional Si atoms were present in the S3 sample, the more Si and C atoms diffused from the SiC substrate, the more vigorous the reaction between C atoms and Ti atoms. The effect of the annealing treatment on the RMS and the thickness of the electrode was larger. Compared with these of the S1 sample, the RMS and thickness increase were 17 nm and 30 nm for S3, respectively. It was reported that the surface morphology of the electrodes affected the electrical properties, and the smoother morphology was beneficinal to the ohmic behavior.[28–32] On the other hand, the Ti_3SiC_2 and $Ti_5Si_3C_x$ were electrically and thermally more highly conductive than TiC which was also beneficial to the formation of good ohmic contact.[33] The experimental and theoretical analysis demonstrates that an ohmic contact with low specific resistivity is related to the smoother surface morphology, and rectifying contact is related to the rough surface morphology.

4. Conclusions

In conclusion, we have grown Ti electrodes on an n-type 4H-SiC by magnetron sputtering and studied the contact properties using TLM measurement. The electrode placement method in the annealing treatment played a key role in the formation of ohmic contact on Ti/4H-SiC. Ohmic contact was achieved when the electrodes were faced to the Si tray. The additional silicon dissociation from the Si tray is the reason why the Ti_3SiC_2 and $Ti_5Si_3C_x$ phases were formed in the electrode surface in S2. The improved smooth surface morphology is a key role in the formation of ohmic contact.

References

[1] Vix-Guterl C, Alix I, Gibot P and Ehrburger P 2003 *Appl. Surf. Sci.* **329** 1639
[2] Katsuno T, Watanabe Y, Fujiwara H, Konishi M, Naruoka H, Morimoto J, Morino T and Endo T 2011 *Appl. Phys. Lett.* **98** 222111
[3] Morkoc H, Strite S, Gao G B, Lin M E, Sverdlov B and Burns M 1994 *J. Appl. Phys.* **76** 1363
[4] Guo H, Zhang Y M, Qiao D Y, Sun L and Zhang Y M 2007 *Chin. Phys.* **16** 1753
[5] Yang H, Peng T H, Wang W J, Zhang D F and Chen X L 2007 *Appl. Surf. Sci.* **254** 527
[6] Yang H, Peng T H, Wang W J, Wang W Y and Chen X L 2008 *Appl. Surf. Sci.* **255** 3121
[7] Goesmann F and Schmid-Fetzer R 1995 *Semicond. Technol.* **10** 1652
[8] Goesmann F and Schmid-Fetzer R 1997 *Mater. Sci. Eng. B* **46** 357
[9] Guo H, Zhang Y M and Zhang Y M 2006 *Chin. Phys.* **15** 2142
[10] Xu M S, Hua X B, Peng Y, Yang K, Xia W, Yu G J and Xu X G 2013 *J. Alloys Compd.* **550** 46
[11] Buchholt K, Ghandi R, Domeij M, Zetterling C M, Lu J, Eklund P, Hultman L and Spetz A L 2011 *Appl. Phys. Lett.* **98** 042108
[12] Wang Z, Tsukimoto S, Saito M, Ito K, Murakami M and Ikuhara Y 2009 *Phys. Rev. B* **80** 245303
[13] Drevin-Bazin A, Barbot J F, Alkazaz M, Cabioch T and Beaufort M F 2012 *Appl. Phys. Lett.* **101** 021606
[14] Stoltz S E, Starnberg H I and Barsoum M W 2003 *J. Phys. Chem. Solids.* **64** 2321
[15] Mohney S E, Hull B A, Lin J Y and Crofton J 2002 *Solid State Electron.* **46** 689
[16] Via F L, Roccaforte F, Makhtari A, Raineri V, Musumeci P and Calcagno L 2002 *Microelectronic Engineering* **60** 269
[17] Reeves G K and Harrison H B 1982 *IEEE Electron Device* **3** 111
[18] Lee S H, Park H and Paine D C 2011 *J. Appl. Phys.* **109** 063702
[19] Tsukimoto S, Nitta K, Sakai T, Moriyama M and Murakami M 2004 *J. Electron Mater.* **33** 460
[20] Frazzetto A, Giannazzo F, Nigro R L, Raineri V and Roccaforte F 2011 *J. Phys. D: Appl. Phys.* **44** 255302
[21] Alami J, Eklund P, Emmerlich J, Wilhelmsson O, Jansson U, Högberg H, Hultman L and Helmersson U 2006 *Thin Solid Films* **515** 1731
[22] Johansson L I and Virojanadara C 2011 *Phys. Status Solidi B* **3** 667
[23] Waldrop J R and Grant R W 1993 *Appl. Phys. Lett.* **62** 2685
[24] Kooi B J, Kabel M, Kloosterman A B and Hosson J T M D 1999 *Acta Mater.* **47** 3105
[25] Tong Q Y, Gutjahr K, Hopfe S, GOsele U and Lee T H 1997 *Appl. Phys. Lett.* **70** 1390
[26] Kim D W and Baik H K 2000 *Appl. Phys. Lett.* **77** 1011
[27] Michaelson H B 1997 *J. Appl. Phys.* **48** 4729
[28] Luo B, Ren F, Fitch R C, Gillespie J K, Jenkins T, Sewell J, Via D, Crespo A, Baca A G, Briggs R D, Gotthold D, Birkhahn R, Peres B and Pearton S J 2003 *Appl. Phys. Lett.* **82** 3910
[29] Radhakrishnan G, Adams P M and Speckman D M 2000 *Thin Solid Films* **358** 131
[30] Lan Y L, Lin H C, Liu H H, Lee G Y, Ren F, Pearton S J, Chang M N and Chyi J I 2009 *Appl. Phys. Lett.* **94** 243502
[31] Aboelfotoh M O and Tu K N 1986 *Phys. Rev. B* **34** 2311
[32] Teraji T, Hara S, Okushi H and Kajimura K 1997 *Appl. Phys. Lett.* **71** 689
[33] Pécz B, Tóth L, di Forte-Poisson M A and Vacas J 2003 *Appl. Surf. Sci.* **206** 8